Comparing bioenergetic models for the optimisation of pacing strategy in road cycling

David Sundström, Peter Carlsson, Mats Tinnsten

Department of Quality Technology and Management, Mechanical Engineering and Mathematics, Mid Sweden University, Akademigatan 1, 83125 Östersund, Sweden
e-mail: david.sundstrom@miun.se

Abstract

Road cycling performance is dependent on race tactics and pacing strategy. To optimise the pacing strategy for any race performed with no drafting, a numerical model was introduced, one that solves equations of motion while minimising the finishing time by varying the power output along the course. The power output was constrained by two different hydraulic models: the simpler critical power model for intermittent exercise (CPIE) and the more sophisticated Margaria-Morton model (M-M). These were compared with a constant power strategy (CPS). The simulation of the three different models was carried out on a fictional 75 kg cyclist, riding a 2,000 m course. This resulted in finishing times of 162.4 s, 155.8 s and 159.3 s and speed variances of 0.58 %, 0.26 % and 0.29 % for the CPS, CPIE and M-M simulations respectively. Furthermore, the average power output was 469.7 W, 469.7 W and 469.1 W for the CPS, CPIE and M-M simulations respectively. The M-M model takes more physiological phenomena into consideration compared to the CPIE model and therefore contributes to an optimised pacing strategy that is more realistic. Therefore, the M-M model might be more suitable for future studies on optimal pacing strategy, despite the relatively slower finishing time.

1. Introduction

The last couple of kilometres in a road cycling race is often the most decisive part when it comes to determining the outcome of the race. Depending on the course characteristics and the overall race situation, a range of race tactics may end up being beneficial. Among these potential tactical manoeuvres, the end spurt and the solo break-away attempt are the most frequently used ones. With poor sprinting abilities, the solo break-away seems to be the best tactical manoeuvre. In a solo break-away at the end of the race, the only objective is to finish in the quickest time possible to maximise the probability of winning. In that situation, the pacing strategy may greatly influence performance.

In 1906, Kennelly [1] formulated mathematical relationships between distance and speed for speed records at the time. He was the first to suggest that constant speed is correlated to performance in numerous locomotive sports such as running, cycling and rowing. However in 1974, Keller [2] showed that a constant pace strategy is only optimal for long distances, and that during short distance races, a fast starting strategy improves performance. The fast start minimises the effect of inertia during the acceleration from rest, which over shorter distances constitutes a greater proportion of the total work done and, therefore, has a greater effect on the total race time. There are also empirical results showing that fast start strategies are superior in middle-distance running. Ariyoshi [3], comparing a fast start strategy with a slow start and a constant pace strategy, proved the fast start delivers beneficial $\dot{V}O_2$ kinetics and increases the time to exhaustion. Billat et al. [4] studied 15 middle distance runners performing either an 800 or a 1,500 m race. The results suggested that the athletes control their running speed to maintain the time-limit at the sequential

anaerobic power constant for the first two thirds of the race. This means a fast start with a gradually exponential decrease in speed. Furthermore, this fast start is not an all-out start; instead it has a safety margin from exhaustion, which is believed to be constant for the initial first two-thirds of the race. In contrast, the last one third of the race is described as an all-out sprint. Swain [5] studied pacing strategies by numerical calculations of different conditions of wind and elevation gradients. He concluded that the power output should be increased on uphill and headwind segments, while reduced on downhill and tailwind segments to improve performance. In a study of seven male cyclists riding 16.1 km on a flat course with varying head- and tailwind, Atkinson and Brunskill [6] confirmed the findings of Swain [5] suggesting that a variable power strategy is beneficial for performance when external conditions are changing.

There has also been extensive research into the optimisation of pacing strategies in locomotive sports. De Koning et al. [7] determined the optimal pacing strategy for the 1,000 and 4,000 m track cycling race using iterative simulations. An all-out strategy showed to be optimal in the 1,000 m time-trial discipline, while an all-out start followed by a constant power strategy was optimal in the 4,000 m pursuit. Gordon [8] introduced an analytical optimisation approach using the method of Lagrange multipliers and the critical power concept, resulting in a variable pacing strategy for a course with multiple climbs. Cangley et al. [9] took a different approach by using a full-scale mechanical simulation model and optimal control theory to optimise the pacing strategy. The approach of optimal control in combination with more sophisticated constraints for power output is used in the studies of Dahmen [10] and Dahmen et al. [11]. Their 6-parameter model, constraining power output, is a modification of the 3-parameter critical power model [12]. By computing a field of optimal pacing strategies, Dahmen [13] shows the applicability of optimal pacing strategies for unpredictable circumstances. However, the 6-parameter model mentioned above does not include the fast and slow components of $\dot{V}O_2$ kinetics. A mathematical model called the Margaria-Morton model (M-M model), which was developed through the rigorous studies of Morton [14], accounts for $\dot{V}O_2$ kinetics in addition to the lactic and alactic components of anaerobic work. The M-M model is supplemented with a dynamical constraint for maximum power output, dependent on the remaining glycogen store [15].

The aim of the present study was to determine the optimal pacing strategy when implementing the M-M model and compare the results to the critical power model for intermittent exercise (CPIE) [16] and the constant power strategy (CPS). We study a race situation where the rider has made a break-away at the end of a race, with 2,000 m left to ride.

2. Method

A model for simulating time-trial road cycling and optimising the pacing strategy was implemented into a MATLAB® program. It solves the equations of motion for road cycling and varies the power output to minimise the finishing time.

2.1. Course and rider

The course was built up of 40 cubic splines on the form $y = f(x)$ where f is the spline function, y is the vertical coordinate and x is the horizontal coordinate. The course inclination is expressed as $\alpha = \tan^{-1}\big(f'(x)\big)$, whereas the course curvature radius is expressed as $R = \frac{\left[1+\left(f'(x)\right)^2\right]^{3/2}}{f''(x)}$ [17]. The course profile being investigated had a 2000 m horizontal distance and a total climb of 40 m, equally distributed on four hills. In this study, no environmental wind and no turns were considered in the simulation.

A fictional male rider with the body mass of $m_b = 75$ kg was subject to simulation and optimisation. His total mass, along with the bicycle and other equipment, was m_{tot} and the total mass moment of inertia of the wheels was I_w. Therefore, the total inertia in the direction of travel was $m_s = m_{tot} + I_w/r_w^2$, where r_w was the wheel radius.

2.2. Equations of motion

Equations of motion were built up by expressions for the external forces acting on the rider-bicycle system (Fig. 1). In these motion equations, the rider-bicycle system was treated as a

particle with constant inertia. This particle was set to move along the predetermined course profile by solving the equations of motion numerically from start to finish. The forces acting on the rider-bicycle system were modelled as the propulsive force (F_s), the aerodynamic drag (F_D), the gravitational force (F_g), the rolling resistance (F_{RR}) and the bearing resistance (F_{BR}) in accordance with Martin et al. [18]. In the following paragraphs, all forces are expressed as scalars but act in the directions shown in Fig. 1.

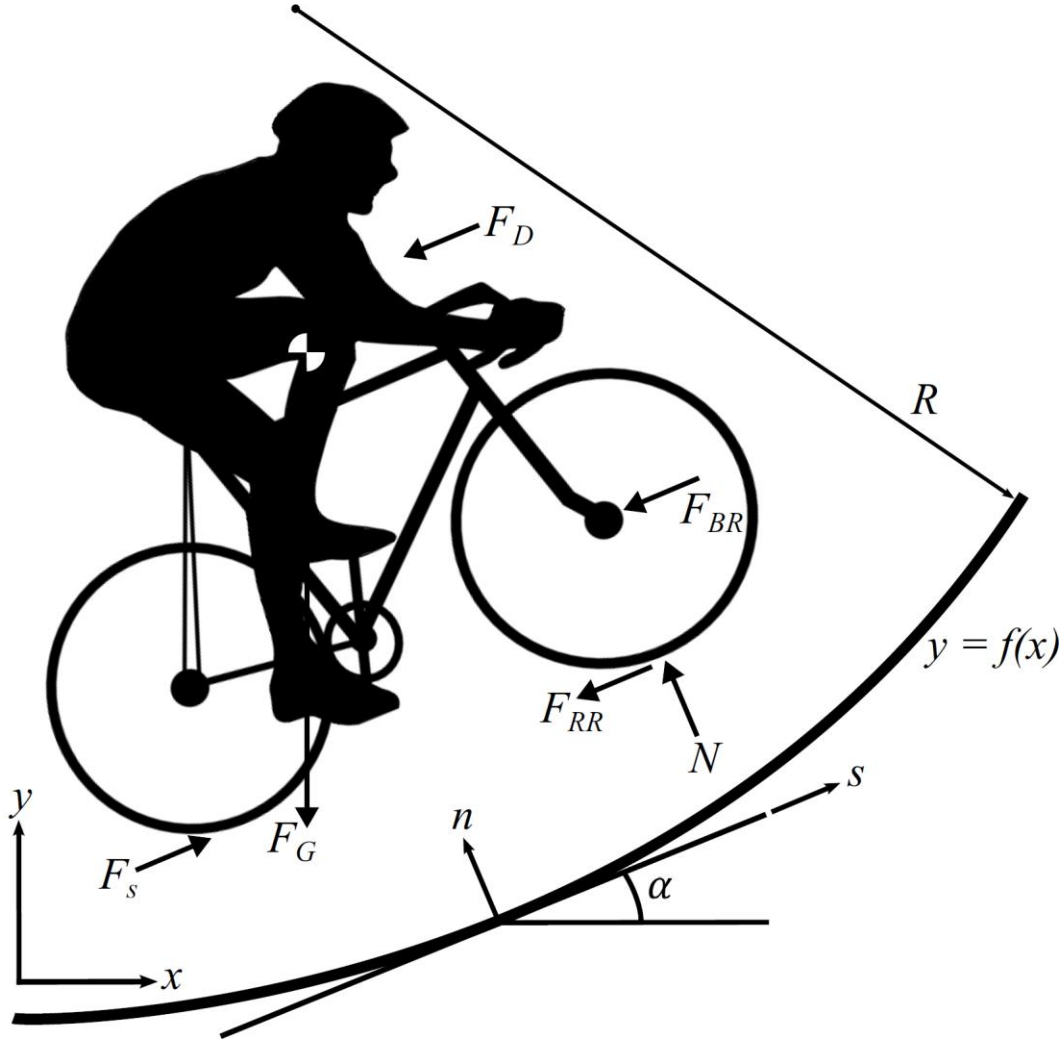

Fig. 1 Arbitrary course section with local and global coordinates, as well as the forces acting on the athlete-bicycle system

The propulsive force acted in the direction of travel and was dependent on the rider's ability to generate power output. Thus, it was expressed as:

$$F_s = P \cdot \eta_{tr} / v \tag{1}$$

where P was the power output generated at the crank spindle, η_{tr} was the mechanical efficiency of the chain transmission and v was the speed parallel to the road. In this study, the drag force was set to be proportional to a constant drag area $C_D A$ and was thus expressed as

$$F_D = \frac{1}{2}(C_D A + A_w)\rho v^2 \tag{2}$$

where A_w is the incremental drag area due to wheel spoke rotation and ρ is the air density. The gravitational force was modelled as:

$$F_g = m_{tot} \cdot g \tag{3}$$

where g is the acceleration of gravity, which may be considered as constant for small vertical and horizontal displacements. The rolling resistance [17,19] was expressed as:

$$F_{RR} = C_{RR} \cdot N = C_{RR} \cdot m_{tot} \left(g \cos \alpha + \frac{v^2}{R} \right) \quad (4)$$

where C_{RR} is the rolling resistance coefficient and N is the normal force acting on the tyres. In addition, the wheel bearing resistance was derived from Dahn et al. [20] and was expressed as:

$$F_{BR} = b_1 + b_2 \cdot v \quad (5)$$

where b_1 and b_2 are constants. The sum of all the external forces was set to perform the acceleration of rider and bicycle.

Equations of motion where developed, with Newton's second law, in the horizontal (x) and vertical (y) directions with all forces [Eqs. (1)-(5)] projected onto these directions. Subsequently, the equations of motion were transformed according to Sundström et al. [21] to make distance (x) the dependant variable and time the independent variable. Consequently, the equation of motion was expressed as:

$$t'' = -(t')^4 \frac{P \cdot \eta_{tr}}{m_s} \cos^2 \alpha + t' \frac{(C_D A + A_W)\rho}{2 \cdot m_s \cos \alpha} + t' \frac{m_{tot}}{m_s} \left[(t')^2 g \cos \alpha \, (C_{RR} \cos \alpha + \sin \alpha) + CRR + \tan \alpha R \cos \alpha + (t')2b1 \cdot t' \cdot \cos \alpha + b2ms \right] \quad (6)$$

where t is time and prime denotes differentiation by x. By introducing a new variable, the motion equation was transformed into a system of first-order ordinary differential equations that could be solved with the 4th order Runge-Kutta method.

2.3. Optimal design

The method of moving asymptotes (MMA) [22,23] was combined with the simulation program to minimise the finishing time (T) while altering power output variables (P_i) along the course. These discrete design variables P_i were distributed with equal spacing in x at 25-m intervals for a total of 81 variables. The power output between these variables was decided by linear interpolation. The numerical optimisation model MMA works in an iterative manner. In each iteration, MMA suggests altered variable values to decrease the objective function, which in this case is the finishing time.

Three different approaches were evaluated for the model's restriction of power output. The first one was a simple CPS where no optimisation was performed. The second approach was the critical power model for intermittent exercise (CPIE) described by Sundström et al. [24], and originally presented by Morton and Billat [16]. The third approach was the M-M model [14], which is described in more detail in this section. A diagrammatical representation of the M-M model can be seen in Figure 2. It is a hydraulic three-component model, in which each vessel volume represents an energy store and the flow of liquid symbolises the energy flow or power. The M-M model consists of three vessels that are connected by three tubes. Vessel O is the aerobic energy store with infinite capacity, vessel AL is the alactic energy store of phosphagens and L is the lactic store of glycogen. Three connection tubes enable one-way flow between the vessels. In tube R_1, liquid flows from vessel O to vessel AL and in tube R_2 liquid flows from vessel L to vessel AL. Tube R_3 is placed at the same level as R_2 but allows liquid to flow in the opposite direction. All three tubes have maximal flow limitations. The maximal flow through tube R_1 is M_O and corresponds to the maximal rate of aerobic energy consumption; R_2 has a maximal flow of M_L which corresponds to the maximal rate of lactic energy consumption; and R_3 has a maximal flow of M_R the maximal rate of lactic restore of glycogen. The magnitude of the present flow through R_1, R_2 and R_3 is decided by the inter-level differences h and l. The lactate threshold is the least power output able to induce a drop in the level of L. The dashed lines in Figure 2 represent the maximal and minimal hydraulic liquid limits in the M-M model. Initially, the liquid level in all vessels was set to the maximal limit. The quantities of H, θ, λ and ϕ in the M-M model are all constants, and the small volume of the narrow tube B was neglected in this study.

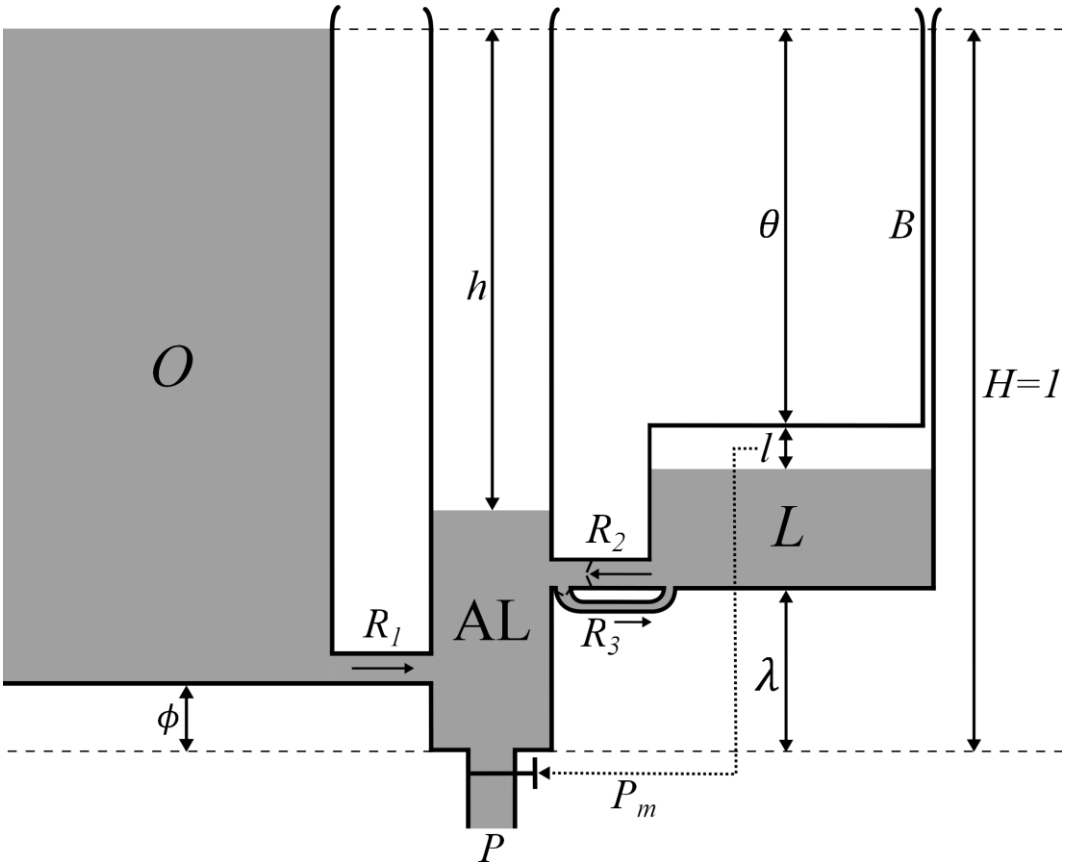

Fig. 2 The Margaria-Morton model with aerobic vessel O, alactic vessel AL and lactic vessel L with the narrow tube B. R_1, R_2 and R_3 are one-way connection tubes (where the flow goes from L to AL in R_2 and from AL to L in R_3) while h and l are the vessel levels in AL and L. P is the power output constrained by the maximal power output P_m. H, ϕ, θ and λ are geometrical parameters of the model

The objective function in the optimisation problem was formulated as:

$$T = \sum_{i=1}^{K} \Delta t_i \tag{7}$$

where K is the total number of discrete distance steps and Δt_i is the time corresponding to each distance step. Furthermore, the constraints for the M-M model were formulated as:

$$0 < \mathrm{AL}_i \leq \mathrm{AL}_{max} \qquad i = 1, \dots, K \tag{8}$$
$$0 < L_i \leq L_{max} \qquad i = 1, \dots, K \tag{9}$$
$$0 \leq P_i \leq P_{m_i} \qquad i = 1, \dots, K \tag{10}$$

The volume in the alactic vessel AL_i and lactic vessel L_i was calculated as:

$$\mathrm{AL}_i = \mathrm{AL}_{i-1} + \left(M_O \frac{h_{i-1}}{H-\phi} + M_L \frac{h_{i-1}-l_{i-1}-\theta}{H-\theta-\lambda} - P_i\right) \Delta t_{i-1} \qquad i = 1, \dots, K \tag{11}$$

$$L_i = L_{i-1} - \left(M_L \frac{h_{i-1}-l_{i-1}-\theta}{H-\theta-\lambda}\right) \Delta t_{i-1} \qquad i = 1, \dots, K \tag{12}$$

However, if $h_{i-1} < l_{i-1} + \theta$, M_L was switched to $-M_R$ in both Eqs. (11) and (12). AL_{max} and L_{max} were the initial and maximal volumes of the alactic and lactic vessels, respectively. Equation (10) was introduced to constrain the rider's power output, in proportion to the level of exertion. The current maximal power output (P_{m_i}) was set to decrease linearly with the level in L [15] and was thus expressed as:

$$P_{m_i} = M_P \frac{H-\theta-\lambda-l_i}{H-\theta-\lambda} \qquad i = 1, \dots, K \tag{13}$$

where M_P is the initial maximal power output, before the level in L starts to fall.

For the assessment of the M-M model, a simpler critical power model was used for comparison. The critical power model for intermittent exercise (CPIE model) [16], as used in the study by Sundström et al. [24], was modelled for this purpose. None of the power output restricting approaches considered the internal work of moving the limbs as there is no consensus about how to calculate this construct accurately [25]. Therefore, we used a constant gross efficiency that compensates for the internal work for constant pedalling frequency.

2.4. Simulation input data

The aim of this study was to determine the optimal pacing strategy for a simple 2-D course of 2,000 m, with four 10-m climbs. The total mass of the rider-bicycle system was calculated to $m_{tot} = 83.9$ kg and the total inertia to $m_s = 85.1$ kg, using an equipment mass of 8.9 kg, a moment of inertia of $I_w = 0.14$ kg·m^2 [18] and a wheel radius of $r_w = 0.337$ m. This rider was set to have a maximal rate of aerobic energy expenditure of 2,000 W corresponding to $\dot{V}O_2\text{max} = 75.8$ ml·kg^{-1}·min^{-1} [26]. Consequently, he had a maximal aerobic power output of $M_O = 450$ W, as the considered gross efficiency was set constantly at 22.5 %, which is in the range of previously reported values [27,28]. The initial maximal power output was set to $M_P = 1{,}100$ W, which is in line with previously reported values on peak power output in sprints [29] and all-out exercise [30]. There are no validated values of M_L, M_R, L_{max} and AL_{max} for this certain rider. Therefore, we chose values, influenced by the findings of Margaria [31] for the maximal lactic power (M_L), the maximal lactic capacity (L_{max}) and the maximal alactic capacity (AL_{max}). Furthermore, on the basis of the M-M model [14], M_R should be much smaller than M_L and M_O. Considering these assumptions, the parameters were set to $M_L = 500$ W, $M_R = 50$ W, $L_{max} = 15{,}000$ J and $\text{AL}_{max} = 7{,}000$ J. The geometrical parameters of the M-M model were set to $\lambda = 0.1$ and $\phi = 0.05$, as proposed by Morton [15], and $\theta = 0.76$ to account for an lactate threshold at 80 % of $\dot{V}O_2max$.

The drag coefficient was taken as $C_D = 0.638$ [32] and the projected frontal area for a break hood's position as $A = 0.562$ m^2 [33] using the scaling laws of Heil. In addition, the supplemental drag area of the wheel spokes was set to $A_w = 0.0044$ m^2, according to Martin et al. [18]. The coefficient of rolling resistance was calculated to $C_{RR} = 0.0042$ [34] using a tyre pressure of 900 kPa and the transmission efficiency of the bicycle was set to $\mu_{tr} = 0.976$ [18]. The bearing friction coefficients were derived from Dahn et al. [20] at $b_1 = 0.089$ and $b_2 = 0.0084$. Furthermore, the starting speed was set at 10 m·s^{-1} to mimic a flying start in the break-away. The air density was set fixed at $\rho = 1.2041$ kg·m^{-3} for 20 °C and 101.325 kPa air pressure; no environmental wind was considered. The optimisation simulation with the M-M model started with all variables set to $P_j = 0.8 \cdot M_O = 360$ W.

The average aerobic power output from the M-M simulation was set as the critical power in the CPIE simulation ($\text{CP} = 372.2$ W). Furthermore, the total anaerobic work produced from both lactic and alactic resources in the M-M simulation was set as the anaerobic work capacity (AWC) in the CPIE simulation ($\text{AWC} = 15{,}440.6$ J). The maximal power output for the CPIE simulation was constant at $P_{m_i} = M_P = 1{,}100$ W and started with all variables set to $P_j = \text{CP}$. All other inputs were equal to the M-M simulation. The even power simulation was performed using a constant power output corresponding to the average power output of the CPIE simulation ($P_j = 469.7$ W).

3. Results

The optimisation routine completed 60 iterations by changing the power output variables. The optimised pacing strategy with the CPIE model and the M-M model is presented in Figs. 3 and 4, respectively. The finishing times were $T_{CPS} = 165.2$ s, $T_{CPIE} = 158.2$ s and $T_{MM} = 159.3$ s. Thus, in comparison with the CPS simulation, the optimisation of the pacing strategy gave time gains of 4.2 and 3.6 % for the CPIE and M-M simulations, respectively. Figure 5 shows the variation of speed for all three approaches to power output restriction. The variances of speed were $var^v_{CPS} = 7.8$ m·s^{-1}, $var^v_{CPIE} = 2.1$ m·s^{-1} and $var^v_{MM} = 5.3$ m·s^{-1} (the speed variance was calculated as $var^v = \frac{1}{K}\sum_{i=1}^{K}(v_i - \bar{v})^2$, where K was the number of distance steps, v_i was the speed at distance step i and $\bar{v}$ was the average speed). Moreover, the maximum speeds were $v^{max}_{CPS} = 16.2$ m·s^{-1}, $v^{max}_{CPIE} = 15.8$ m·s^{-1} and $v^{max}_{MM} = 16.0$ m·s^{-1}. The average power outputs were $\bar{P}_{CPS} = 469.7$ W, $\bar{P}_{CPIE} = 469.7$ W and $\bar{P}_{MM} = 469.1$ W while the variances of power output were $var^P_{CPS} = 0$ W, $var^P_{CPIE} = 6.7{\cdot}10^4$ W and $var^P_{MM} = 2.4{\cdot}10^4$ W (the power output variance was calculated as

$var^P = \frac{1}{K}\sum_{i=1}^{K}(P_i - \bar{P})^2$, where K was the number of distance steps and P_i was the power output at distance step i). Furthermore, the remaining available anaerobic work in the CPIE simulation was 7.0 J (0.045 % of AWC) and the remaining alactic and lactic work in the M-M simulation were AL_K = 1,055.6 J (15 %) and L_K = 5,503.8 J (37 %).

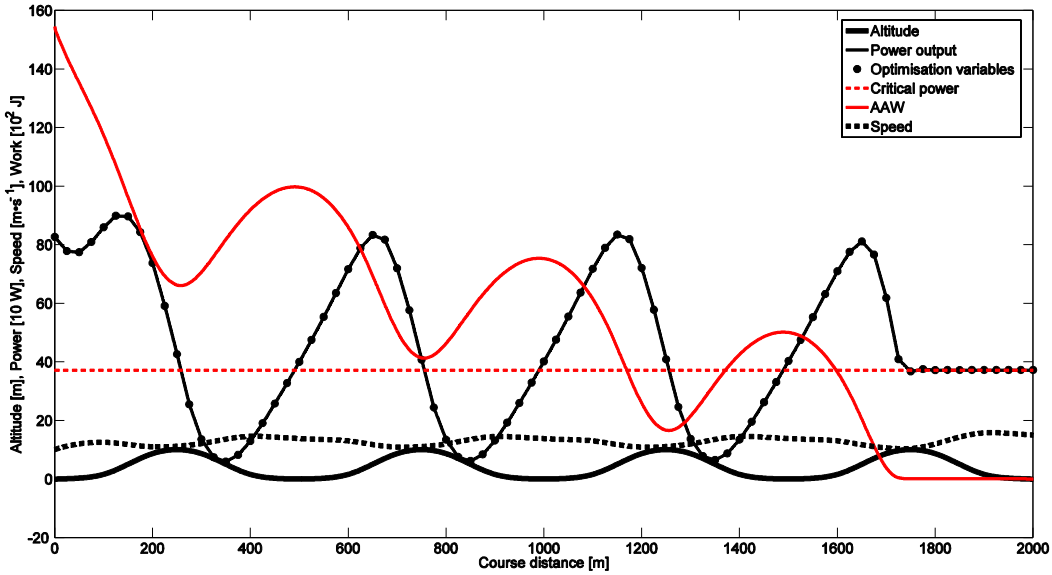

Fig. 3 Optimised pacing strategy constrained by the CPIE model

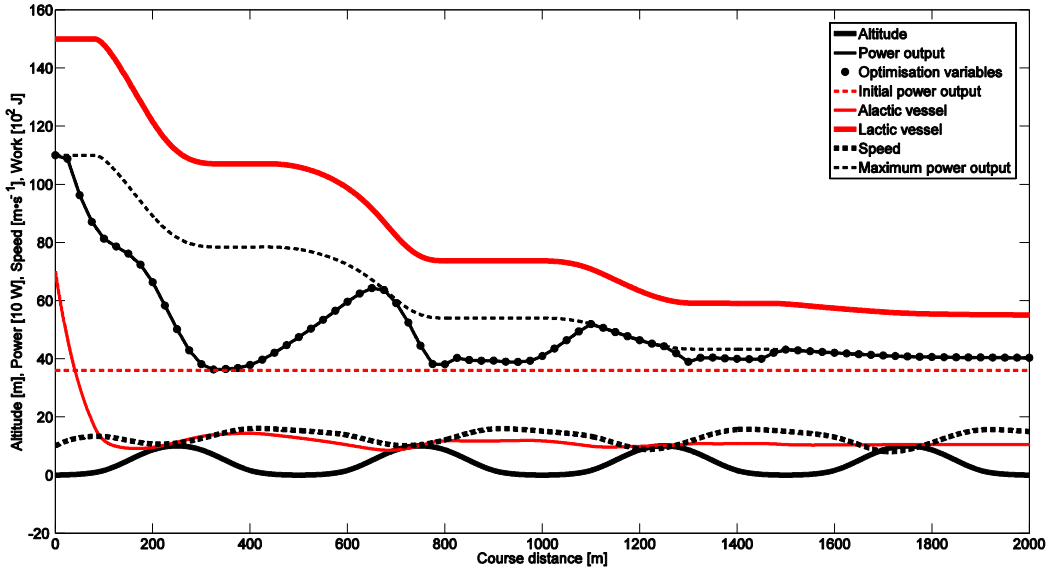

Fig. 4 Optimised pacing strategy constrained by the M-M model

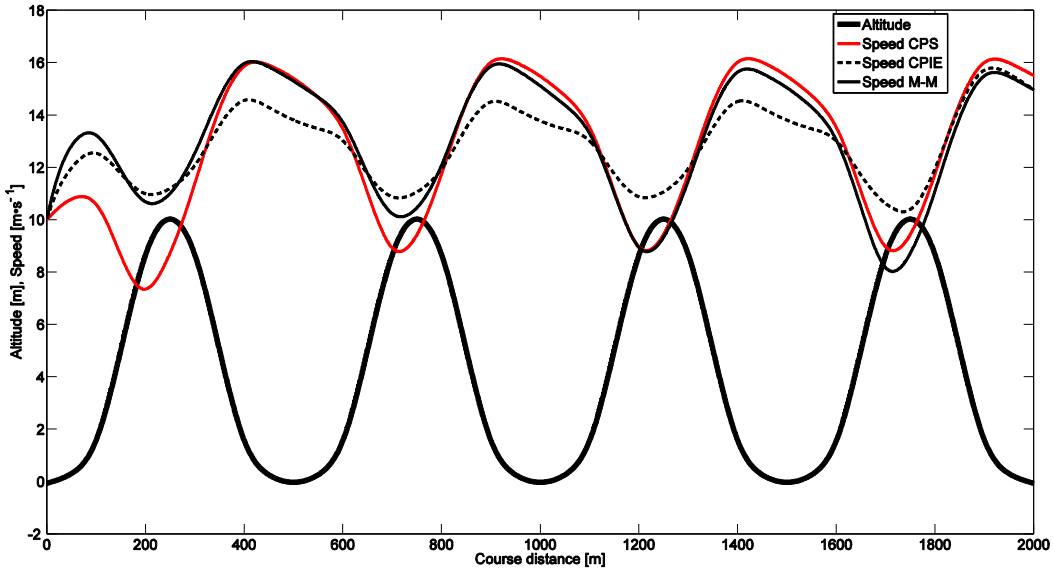

Fig. 5 Speed variations for the three modelling approaches

4. Discussion

Firstly, it was clearly shown in Fig. 5 that the different modelling approaches led to differing pacing strategies. By minimising finishing time, the optimisation worked to reduce the speed variance while still fulfilling the constraints. It is clear that the three different pacing strategies are not equal when it comes to minimising the speed variance.

The initial stage of the course was covered relatively slowly with the CPS, while the optimisation simulations made for faster starts. The M-M simulation had the fastest start, with maximal power output reached immediately. It is of course a good idea to reach average speed as quickly as possible to reduce the speed variance. However, for the M-M model, it is also beneficial to generate a high power output at an early stage to decrease the level in AL, to increase the flow through R_1, ultimately increasing the aerobic contribution to power output. There is empirical evidence showing that the time to reach $\dot{V}O_2max$ is inversely related to exercise intensity [35,36]. In this way, a fast start leads to a higher average power output, which is, of course, beneficial to performance. Furthermore, the findings of the fast start being optimal are consistent with the findings of Keller [2], Ariyoshi [3] and de Koning et al. [7]. Additionally, Morton et al. [37] concluded that any bioenergetic model with a maximum power feedback coupling, dependent on a monotonically decreasing fashion on the amount of fuel substrate remaining, would require all-out effort for optimal performance. This would suggest an all-out effort ($P_\mathrm{i} = P_{m_i}$) for the entire course distance in the M-M simulation. However, due to the gravity and the hills considered in the present study, optimal performance required part-wise all-out effort in the M-M simulation. A similar maximum power constraint applied in the M-M model is suggested by Morton [38] for the critical power model; however, it was not considered in this study.

In the middle stages of the course, between the first and last summits, the pacing strategies for CPS and CPIE had periodically recurrent variations in speed, which was a result of the constant and periodic behaviour of the power output distributions (Fig. 3). Conversely, the speed variation in the M-M simulation had a decreasing trend as a result of the stagnation in power output (Fig. 4) due to the maximal power constraint in Eqs. (10) and (13). This constrained power output seems very intuitive as the maximal producible power output really is constrained at high exertion. However, it also seems like the maximal power constraint was largely responsible for the large remaining volumes AL_K (15 %) and L_K (37 %) at the finish line. This indicates that the rider was not exhausted, but Eqs. (10) and (13) would not allow a power output that is sufficient to empty any of the anaerobic vessels. Therefore, future work may develop the M-M model [15] to incorporate a modified maximum power constraint. Overall, the variations in power output, seen in the middle stages of the course for the optimised simulations, are supported by the theoretical study of Swain [5] and the empirical study of Atkinson and Brunskill [6], showing that the power output should be altered to meet the external conditions, such as the course inclination. Although these variations in power output are to the largest extent a result of the varying altitude, St Clair

Gibson and Noakes [39] suggest that the central governor itself, induces oscillatory variations in exercise intensity. This central governor theory is based on integrative central neural regulation of effort and fatigue in exercising humans [40]. By sensing physiological changes, the central nervous system regulates the recruitment of motor units to retain homeostasis. The oscillatory governed exercise intensity is a result of the dynamical process in a complex system with different peripheral and central, feedback and feedforward systems. Though the central governor model in humans is realistic, no study to date has shown that this natural pacing with oscillatory exercise intensity is optimal for constant external conditions.

In the final stage of the course, from the last summit to the finish, there were similar pacing strategies in all three simulations (Fig. 5), indicating a minor correlation between modelling approaches and pacing in the final stage. The overall speed variance clearly showed a relation to the finishing time. The lower the speed variance, the lower finishing time was obtained. This is a logical consequence of the drag force's dependence upon the squared speed (Eq. 2).

The results of the present study showed that the CPIE simulation yielded the fastest pacing strategy. However, it is conceivable to assume that the M-M model better describes the real human body's restriction of power output. The fast and slow components of $\dot{V}O_2$ kinetics are considered in the M-M model while completely omitted in the CPIE model. It has also been shown that the rate of refuelling the anaerobic energy stores in real athletes is not described by a linear function of time, but rather an exponential time course [41]. Furthermore, if we consider the power output generated in the CPIE simulation in the last uphill (Fig. 3) it is not likely that the simulated rider would really generate such high power output with an almost emptied storage of anaerobic work. In this case, the M-M model performed a more realistic pacing strategy, where the rider's ability to generate power output declined with the decline in the lactic energy store.

The type of optimisation problem posed for the M-M model makes it impossible to use a convergence criterion. The dynamical constraint in Eq. (10) is very sensible to variable values. A small alteration in one variable, caused by a small computational error, may affect the constraint to be violated by another variable, resulting in an infeasible solution. Therefore, an equal number of iterations were performed to compare the different bioenergetic models. Among these iterations, the feasible solution with the lowest objective function value was chosen as the optimum. Furthermore, the improvement in the objective function between the last two feasible iterations in the CPIE simulation was less than 0.03 s and for the M-M simulation the same number was less than 0.09 s. This suggests that further iterations would only result in small improvements.

Solo break-away attempts do not solely benefit from minimising the time to finish. For instance, the perceived distance to another competitor may influence motivation for further exertion, thus a fast start strategy may be favourable to demoralise one's competitors.

5. Conclusions

The CPIE model created a pacing strategy that was 0.68 % faster than the strategy constrained by the M-M model. However, the M-M model has a more realistic restriction on the rider's power output including the dynamic restriction of aerobic work rate as well as lactic work rate, and of course the dynamic constraint on the power output. Furthermore, this includes the limits of anaerobic work capacity for different substrates. According to this, the M-M model yielded an optimised pacing strategy that is more realistic than the one obtained from the CPIE model. Therefore, it is conceivable to assume that the M-M model is preferable in comparison to the CPIE model, for the application of optimal pacing strategies in real-world competition. However, this has to be confirmed through validation studies performed on real riders, which is not within the scope of the present study. Nevertheless, variable pacing strategies, including the ones derived from the CPIE and M-M simulations, had faster finishing times than the CPS simulation on a hilly course.

Acknowledgements

This work was supported by the European Regional Development Fund of the European Union.

Conflict of interest

The authors declare that they have no conflict of interest.

References

1. Kennelly AE (1906) An approximate law of fatigue in the speeds of racing animals. Proceedings of the American Academy of Arts and Sciences 42:275-331.
2. Keller JB (1974) Optimal Velocity in a Race. Am Math Mon 81:474-480. doi: 10.2307/2318584
3. Ariyoshi M, Yamaji K, Shephard RJ (1979) Influence of running pace upon performance: effects upon treadmill endurance time and oxygen cost. Eur J Appl Physiol Occup Physiol 41:83-91.
4. Billat V, Hamard L, Koralsztein JP, Morton RH (2009) Differential modeling of anaerobic and aerobic metabolism in the 800-m and 1,500-m run. J Appl Physiol 107:478-487. doi: 10.1152/japplphysiol.91296.2008
5. Swain DP (1997) A model for optimizing cycling performance by varying power on hills and in wind. Med Sci Sport Exer 29:1104-1108. doi: 10.1097/00005768-199708000-00017
6. Atkinson G, Brunskill A (2000) Pacing strategies during a cycling time trial with simulated headwinds and tailwinds. Ergonomics 43:1449-1460. doi: 10.1080/001401300750003899
7. de Koning JJ, Bobbert MF, Foster C (1999) Determination of optimal pacing strategy in track cycling with an energy flow model. J Sci Med Sport 2:266-277. doi: 10.1016/S1440-2440(99)80178-9
8. Gordon S (2005) Optimising distribution of power during a cycling time trial. Sports eng 8:81-90. doi: 10.1007/bf02844006
9. Cangley P, Passfield L, Carter H, Bailey M (2011) The effect of variable gradients on pacing in cycling time-trials. Int J Sports Med 32:132-136. doi: 10.1055/s-0030-1268440
10. Dahmen T Optimization of pacing strategies for cycling time trials using a smooth 6-parameter endurance model. In: Pre-Olympic Congress on Sports Science and Computer Science in Sport (IACSS2012), Liverpool, UK, 2012. IACSS Press.
11. Dahmen T, Saupe D, Wolf S Applications of mathematical models of road cycling. In: Vienna International Conference on Mathematical Modelling (MATHMOD), Vienna, Austria, 2012.
12. Morton RH (2006) The critical power and related whole-body bioenergetic models. Eur J Appl Physiol 96:339-354. doi: 10.1007/s00421-005-0088-2
13. Dahmen T Computing a field of optimal pacing strategies for cycling time trials. In: Symposium der dvs-Sektion Sportinformatik, Konstanz, Germany, 2012.
14. Morton RH (1986) A three component model of human bioenergetics. J Math Biol 24:451-466.
15. Morton RH (1990) Modelling human power and endurance. J Math Biol 28:49-64.
16. Morton RH, Billat LV (2004) The critical power model for intermittent exercise. Eur J Appl Physiol 91:303-307. doi: 10.1007/s00421-003-0987-z
17. Meriam JL, Kraige LG (2013) Engineering Mechanics Dynamics SI version. 7 edn. John Wiley and Sons, Singapore.
18. Martin JC, Milliken DL, Cobb JE, McFadden KL, Coggan AR (1998) Validation of a mathematical model for road cycling power. J Appl Biomech 14:276-291.
19. Meriam JL, Kraige LG (2013) Engineering Mechanics Statics SI version. 7 edn. John Wiley and Sons, Singapore.
20. Dahn K, Mai L, Poland J, Jenkins C (1991) Frictional resistance in bicycle wheel bearings. Cycling Science 3:28-32.
21. Sundström D, Carlsson P, Ståhl F, Tinnsten M (2013) Numerical optimization of pacing strategy in cross-country skiing. Struct Multidisc Optim 47:943-950. doi: 10.1007/s00158-012-0856-7
22. Svanberg K (1987) The method of moving asymptotes - a new method for structural optimization. Int J Numer Meth Eng 24:359-373. doi: 10.1002/nme.1620240207
23. Svanberg K (1993) The method of moving asymptotes (MMA) with some extensions. Optimization of Large Structural Systems, Vols 1 231:555-566.
24. Sundström D, Carlsson P, Tinnsten M On optimization of pacing strategy in road cycling. In: 6th Asia-Pacific Congress on Sports Technology (APCST), Hong Kong, 2013. Elsevier.
25. Minetti AE (2011) Bioenergetics and biomechanics of cycling: the role of 'internal work'. Eur J Appl Physiol 111:323-329. doi: 10.1007/s00421-010-1434-6
26. McArdle WD, Katch FI, Katch VL (2010) Exercise physiology: nutrition, energy, and human performance. 7 edn. Lippincott Williams and Wilkins, Baltimore.

27. Coyle EF, Sidossis LS, Horowitz JF, Beltz JD (1992) Cycling efficiency is related to the percentage of type I muscle fibers. Med Sci Sport Exer 24:782-788.
28. Lucia A, Juan AFS, Montilla M, Canete S, Santalla A, Earnest C, Perez M (2004) In professional road cyclists, low pedaling cadences are less efficient. Med Sci Sport Exer 36:1048-1054. doi: Doi 10.1249/01.Mss.0000128249.10305.8a
29. Del Coso J, Mora-Rodriguez R (2006) Validity of cycling peak power as measured by a short-sprint test versus the Wingate anaerobic test. Applied Physiology Nutrition and Metabolism - Physiologie Appliquee Nutrition Et Metabolisme 31:186-189. doi: 10.1139/H05-026
30. Brickley G, Dekerle J, Hammond AJ, Pringle J, Carter H (2007) Assessment of maximal aerobic power and critical power in a single 90-s isokinetic all-out cycling test. Int J Sports Med 28:414-419. doi: 10.1055/s-2006-924513
31. Margaria R, Margaria R (1976) Biomechanics and energetics of muscular exercise. Clarendon Press Oxford.
32. Heil DP (2001) Body mass scaling of projected frontal area in competitive cyclists. Eur J Appl Physiol 85:358-366.
33. Heil DP (2002) Body mass scaling of frontal area in competitive cyclists not using aero-handlebars. Eur J Appl Physiol 87:520-528. doi: 10.1007/s00421-002-0662-9
34. Grappe F, Candau R, Barbier B, Hoffman MD, Belli A, Rouillon JD (1999) Influence of tyre pressure and vertical load on coefficient of rolling resistance and simulated cycling performance. Ergonomics 42:1361-1371. doi: 10.1080/001401399185009
35. Jones AM, Wilkerson DP, Vanhatalo A, Burnley M (2008) Influence of pacing strategy on O2 uptake and exercise tolerance. Scandinavian Journal of Medicine and Science in Sports 18:615-626. doi: 10.1111/j.1600-0838.2007.00725.x
36. Hill DW, Ferguson CS (1999) A physiological description of critical velocity. Eur J Appl Physiol O 79:290-293. doi: 10.1007/s004210050509
37. Morton RH (2009) A new modelling approach demonstrating the inability to make up for lost time in endurance running events. Ima J Manag Math 20:109-120. doi: 10.1093/imaman/dpn022
38. Morton RH (1996) A 3-parameter critical power model. Ergonomics 39:611-619. doi: 10.1080/00140139608964484
39. St Clair Gibson A, Noakes TD (2004) Evidence for complex system integration and dynamic neural regulation of skeletal muscle recruitment during exercise in humans. Br J Sports Med 38:797-806. doi: 10.1136/bjsm.2003.009852
40. Noakes TD, Gibson AS, Lambert EV (2005) From catastrophe to complexity: a novel model of integrative central neural regulation of effort and fatigue during exercise in humans: summary and conclusions. Brit J Sport Med 39:120-124. doi: 10.1136/bjsm.2003.010330
41. Skiba PF, Chidnok W, Vanhatalo A, Jones AM (2012) Modeling the expenditure and reconstitution of work capacity above critical power. Med Sci Sports Exerc 44:1526-1532. doi: 10.1249/MSS.0b013e3182517a80